Electronic Supplementary Material (ESI) for CrystEngComm.

Systematic Arrangement Control of Functional Organic Molecules

Ryota Akai,† Kouki Oka,† Ryunosuke Nishida, Norimitsu Tohnai*

Department of Applied Chemistry and Center for Future Innovation (CFi), Graduate School of Engineering, Osaka University, 2-1 Yamadaoka, Suita, Osaka 565-0871, Japan.
Email: tohnai@chem.eng.osaka-u.ac.jp (Norimitsu Tohnai)

† R.A. and K.O. contributed equally to this work.

Experimental Sections

Materials.

Hydrochloric acid was purchased from Kishida Chemical Co., Ltd. Bis(pinacolate)diboron, 4-bromobenzenesulfonyl chloride, 5,5'-dibromo-2,2'-bithiophene, isobutylamine, methyltri-*n*-octylammonium chloride, butylamine, neopentyl alcohol, *sec*-butylamine, *tert*-butylamine, α-terthiophene, (4,4,5,5-tetramethyl-1,3,2-dioxaborolan-2-yl)benzene were purchased from Tokyo Chemical Industry Co, Ltd. Other chemicals were purchased from FUJIFILM Wako Pure Chemical Corporation.

Measurements.

Proton nuclear magnetic resonance (^{1}H NMR) spectra were recorded by a JEOL 400 JJYH (400 MHz) spectrometer with chemical shifts downfield from tetramethylsilane as the internal standard. Carbon nuclear magnetic resonance (^{13}C NMR) spectra were recorded by a JEOL 400 JJYH (400 MHz) spectrometer with chemical shifts downfield from tetramethylsilane as the internal standard. The X-ray diffraction data of the organic salts were collected on a two-dimensional X-ray detector (PILATUS 200 K/R) equipped in Rigaku XtaLAB PRO diffractometer using thin multi-layer mirror monochromated Cu-Kα radiation (λ = 1.54187 Å).

The cell refinements were performed with CrysAlisPro a software 1.171.39.5. SHELXT was used for the structure solution of the crystals. All calculations were performed with the observed reflections [$I>2\sigma(I)$] with the program CrystalStructure crystallographic software packages, except for refinement which was performed by SHELXL. All non-hydrogen atoms were refined with anisotropic displacement parameters, and hydrogen atoms were placed in idealized positions and refined as rigid atoms with the relative isotropic displacement parameters. Powder X-ray diffraction (PXRD) was performed with a Rigaku Ultima IV using graphite monochromatized Cu-Kα radiation (λ = 1.54187 Å) at 25°C. Thermogravimetric analysis were performed with a TG-DTA8122 (Rigaku) at a heating rate of 3°C min^{-1} under nitrogen. Differential scanning calorimetry were performed with a DSC vesta Thermo plus EVO2 (Rigaku) at a heating rate of 3°C min^{-1} under nitrogen. ATR-IR spectra were performed using on an IRT-5000_FT/IR-4200 (JASCO). Measurements of fluorescence excitation and emission spectra were performed using a FP-8500 spectrofluorometer (JASCO). Fluorescence quantum efficiencies were performed using a FP-8500 spectrofluorometer (JASCO) with an ISF-834 fluorescence integrate sphere unit (JASCO). The excitation wavelength was 340 nm. Measurements of UV-Vis absorption spectra were performed using a V-770 spectrophotometer (JASCO).

Fluorescence lifetime measurements for the crystals were performed using a TemPro Fluorescence Lifetime System (Horiba Jobin Yvon) equipped with an LED excitation source of 352 nm with a pulse-duration full width at half maximum (FWHM) of approximately 1 ns.

Synthesis of neopentyl 4-bromobenzenesulfonate.

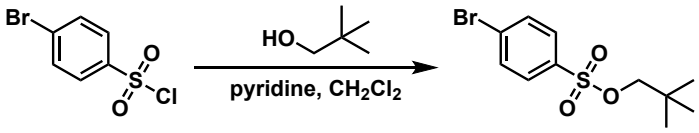

Scheme S1. Synthesis of neopentyl 4-bromobenzenesulfonate.

We synthesized neopentyl 4-bromobenzenesulfonate following the previous report[1]. 4-Bromobenzene-1-sulfonyl chloride (50.4 g, 197 mmol) was added to pyridine (18.7 g, 237 mmol), and then neopentyl alcohol (20.8 g, 236 mmol) in CH_2Cl_2 (50 mL) was dropped into the mixture at 0°C. The mixture was stirred at 0°C for 2 h, and then was stirred at 25°C for 24 h. After the reaction, the resulting mixture was concentrated in vacuo, and CH_2Cl_2 was added to the residue. The organic layer was washed with 0.5 M aqueous HCl, saturated $NaHCO_3$ solution, water, and brine, and was concentrated in vacuo. The crude was purified by recrystallization in *n*-hexane to give a white powder of neopentyl 4-bromobenzenesulfonate (39.8 g, 65%, Figure S6): ^{1}H NMR (400 MHz, chloroform-d_1, δ): 7.8 (m, 2H), 7.7 (m, 2H), 3.7 (s, 2H), 0.9 (s, 9H).

Synthesis of neopentyl 4-(4,4,5,5-tetramethyl-1,3,2-dioxaborolan-2-yl)benzenesulfonate.

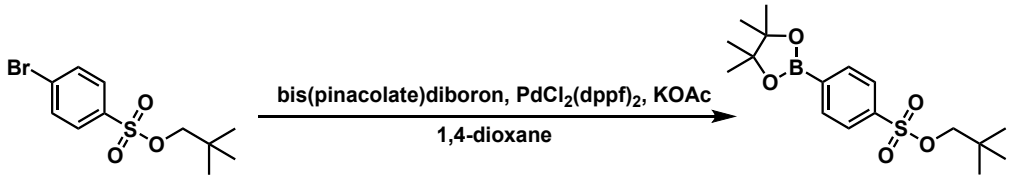

Scheme S2. Synthesis of neopentyl 4-(4,4,5,5-tetramethyl-1,3,2-dioxaborolan-2-yl)benzenesulfonate.

We synthesized neopentyl 4-(4,4,5,5-tetramethyl-1,3,2-dioxaborolan-2-yl)benzenesulfonate following the previous report[1]. Neopentyl 4-bromobenzenesulfonate (5.05 g, 16.4 mmol), bis(pinacolate)diboron (5.05 g, 19.9 mmol), $PdCl_2(dppf)_2$ (0.242 g, 0.331 mmol), and KOAc (4.77 g, 48.6 mmol) were added to 1,4-dioxane (115 mL) under nitrogen, and then the mixture was stirred at 120°C for 24 h. After the reaction, the resulting mixture was concentrated in vacuo, and ethyl acetate was added to the residue. The organic layer was filtered and washed with saturated $NaHCO_3$ solution, water, and brine, and dried over anhydrous $MgSO_4$. After evaporation of the solvent, the residue was purified by flash column chromatography on silica gel with $CHCl_3$ as the eluent. The crude was purified by recrystallization in 2-propanol to give a white solid of neopentyl 4-(4,4,5,5-tetramethyl-1,3,2-dioxaborolan-2-yl)benzenesulfonate (4.60, 80%, Figure S7): ^{1}H NMR (400

MHz, chloroform-d_1, δ): 8.0 (m, 2H), 7.9 (m, 2H), 3.7 (s, 2H), 1.4 (s, 12H), 0.9 (s, 9H).

Synthesis of dineopentyl 4,4'-([2,2'-bithiophene]-5,5'-diyl)dibenzenesulfonate.

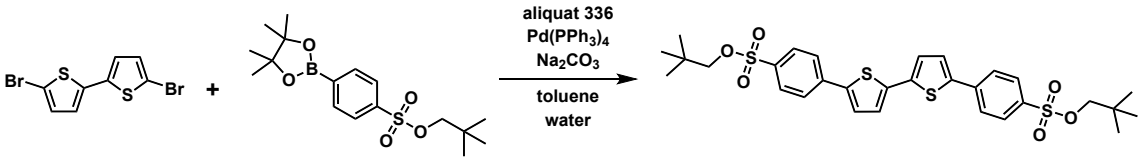

Scheme S3. Synthesis of dineopentyl 4,4'-([2,2'-bithiophene]-5,5'-diyl)dibenzenesulfonate.

Neopentyl 4-(4,4,5,5-tetramethyl-1,3,2-dioxaborolan-2-yl)benzenesulfonate (2.73 g, 7.72 mmol), 5,5'-dibromo-2,2'-bithiophene (1.00 g, 3.09 mmol), tetrakis(triphenylphosphine)palladium(0) (0.360 g, 0.312 mmol), aliquat 336 (0.120 g, 0.297 mmol), and anhydrous Na_2CO_3 (3.27 g, 30.9 mmol) were added to toluene (50 mL) and water (20 mL) under nitrogen, and the mixture was refluxed at 90°C for 26 h. After the reaction, the reaction mixture was concentrated in vacuo, and was extracted with ethyl acetate. The organic layer was washed with water and brine, and evaporated under vacuum. The residue was washed with CH_2Cl_2 (15 mL × 2) to give a yellow solid. This solid was characterized as dineopentyl 4,4'-([2,2'-bithiophene]-5,5'-diyl)dibenzenesulfonate (1.64 g, 86%), as follows (Figures S8 and S9): ^{1}H NMR (400 MHz, chloroform-d_1, δ): 7.9 (m, 4H), 7.8 (m, 4H), 7.4 (d, 2H, J = 3.6 Hz), 7.3 (2H), 3.7 (s, 4H), 0.9 (s, 18H); ^{13}C NMR (400 MHz, chloroform-d_1, δ): 141.1, 138.9, 138.3, 134.5, 128.8, 126.2, 125.8, 125.4, 79.8, 31.7, 26.0.

Synthesis of 4,4'-([2,2'-bithiophene]-5,5'-diyl) dibenzenesulfonic acid (BTDBS).

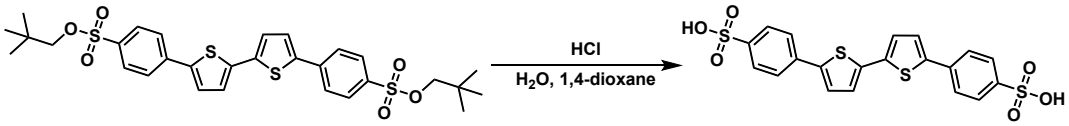

Scheme S4. Synthesis of 4,4'-([2,2'-bithiophene]-5,5'-diyl)dibenzenesulfonic acid (**BTDBS**).

Dineopentyl 4,4'-([2,2'-bithiophene]-5,5'-diyl)dibenzenesulfonate (1.60 g, 2.59 mmol), 2 M HCl aqueous solution (40 mL) was added to 1,4-dioxane (160 mL), and the mixture was stirred at 120°C for 68 h. After the reaction, the resulting mixture was concentrated in vacuo to give oily crude. Dimethyl sulfoxide was added to the crude, and the solution was reprecipitated from diethyl ether to give a yellow solid. The solid was characterized as 4,4'-([2,2'-bithiophene]-5,5'-diyl)dibenzenesulfonic acid (**BTDBS**), as follows (Figures S10 and S11): ^{1}H NMR (400 MHz, dimethyl sulfoxide-d_6, δ): 7.6 (m, 8H), 7.5 (d, 2H, J = 4.0 Hz), 7.4 (d, 2H, J = 4.0 Hz); ^{13}C NMR (400 MHz, dimethyl sulfoxide-d_6, δ): 147.7, 141.8, 135.8, 133.1, 126.4, 125.4, 125.2, 124.5.

Preparation of the organic salt composed of 4,4'-([2,2'-bithiophene]-5,5'-diyl) dibenzenesulfonic acid and nBuA (BTDBS/nBuA).

The **BTDBS** crude (0.323 mmol), just after the hydrolysis of dineopentyl 4,4'-([2,2'-bithiophene]-5,5'-diyl)dibenzenesulfonate, was dissolved in ethanol (40 mL) to give slurry solution. Then, ***n*BuA** (740 mg, 10.1 mmol) was added to the solution, and then the mixture was stirred at 25°C for 18 h. After the reaction, the mixture was filtered, and then the residue was washed with diethyl ether (20 mL × 3). The **BTDBS/*n*BuA** (187 mg, 0.299 mmol) was obtained as a yellow powder.

Preparation of the single crystals of 4,4'-([2,2'-bithiophene]-5,5'-diyl)dibenzenesulfonic acid and nBuA (BTDBS/nBuA).

The organic salt of **BTDBS/*n*BuA** (1.0 mg) was dissolved in methanol (500 μL). Then, *n*-decane (500 μL) as poor solvent was added to the solution. Slow evaporation of the solvent at 25°C gave the single crystals of **BTDBS/*n*BuA**.

Preparation of the organic salt composed of 4,4'-([2,2'-bithiophene]-5,5'-diyl)dibenzenesulfonic acid and isoBuA (BTDBS/isoBuA).

The **BTDBS** crude (0.323 mmol), just after the hydrolysis of dineopentyl 4,4'-([2,2'-bithiophene]-5,5'-diyl)dibenzenesulfonate, was dissolved in ethanol (40 mL) to give slurry solution. Then, **isoBuA** (740 mg, 10.1 mmol) was added to the solution, and then the mixture was stirred at 25°C for 18 h. After the reaction, the mixture was filtered, and then the residue was washed with diethyl ether (20 mL × 3). The **BTDBS/isoBuA** (188 mg, 0.301 mmol) was obtained as a yellow powder.

Preparation of the single crystals of 4,4'-([2,2'-bithiophene]-5,5'-diyl)dibenzenesulfonic acid and isoBuA (BTDBS/isoBuA).

The organic salt of **BTDBS/isoBuA** (1.0 mg) was dissolved in methanol (500 μL). Then, toluene (250 μL) as poor solvent was added to the solution. Slow evaporation of the solvent at 25°C gave the single crystals of **BTDBS/isoBuA**.

Preparation of the organic salt composed of 4,4'-([2,2'-bithiophene]-5,5'-diyl)dibenzenesulfonic acid and sBuA (BTDBS/sBuA).

The **BTDBS** crude (0.323 mmol), just after the hydrolysis of dineopentyl 4,4'-([2,2'-bithiophene]-5,5'-diyl)dibenzenesulfonate, was dissolved in ethanol (40 mL) to give slurry solution. Then, ***s*BuA** (740 mg, 10.1 mmol) was added to the solution, and then the mixture was stirred at 25°C for 18 h. After the reaction, the mixture was filtered, and then the residue was washed with diethyl ether (20 mL × 3). The **BTDBS/*s*BuA** (133 mg, 0.213 mmol) was obtained as a yellow powder.

Preparation of the single-crystals of 4,4'-([2,2'-bithiophene]-5,5'-diyl)dibenzenesulfonic acid and sBuA (BTDBS/sBuA).

The organic salt of **BTDBS/*s*BuA** (1.0 mg) was dissolved in methanol (500 μL). Then, *n*-decane (250 μL) as poor solvent was added to the solution. Slow evaporation of the solvent at 25°C gave the single crystals of **BTDBS/*s*BuA**.

Synthesis of 5,5'-diphenyl-2,2'-bithiophene (DPhBT).

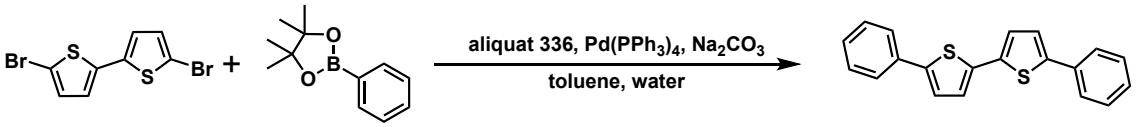

Scheme S5. Synthesis of 5,5'-diphenyl-2,2'-bithiophene (**DPhBT**).

(4,4,5,5-Tetramethyl-1,3,2-dioxaborolan-2-yl)benzene (157 mg, 0.771 mmol), 5,5'-dibromo-2,2'-bithiophene (100 mg, 0.309 mmol), tetrakis(triphenylphosphine)palladium(0) (36.0 mg, 0.0309 mmol), aliquat 336 (120 mg, 0.297 mmol), and anhydrous Na_2CO_3 (327 mg, 3.09 mmol) were added to toluene (20 mL), and water (10 mL) under nitrogen, and the mixture was refluxed at 100°C for 22 h. After the reaction, toluene was added to the reaction mixture, and the organic layer was washed with water and brine, and dried over anhydrous $MgSO_4$. After evaporation of the solvent, the residue was washed with *n*-hexane (30 mL). The washed residue was dried to give a yellow solid of 5,5'-diphenyl-2,2'-bithiophene (**DPhBT**) (87.0 mg, 89%, Figures S12 and S13). ^{1}H NMR (400 MHz, chloroform-d_1, δ): 7.6 (m, 4H), 7.4 (m, 4H), 7.3 (m, 2H), 7.2 (d, 2H, J = 4.0 Hz), 7.2 (d, 2H, J = 3.6 Hz); ^{13}C NMR (400 MHz, chloroform-d_1, δ): 143.1, 136.7, 134.0, 128.9, 127.6, 125.6, 124.5, 123.8.

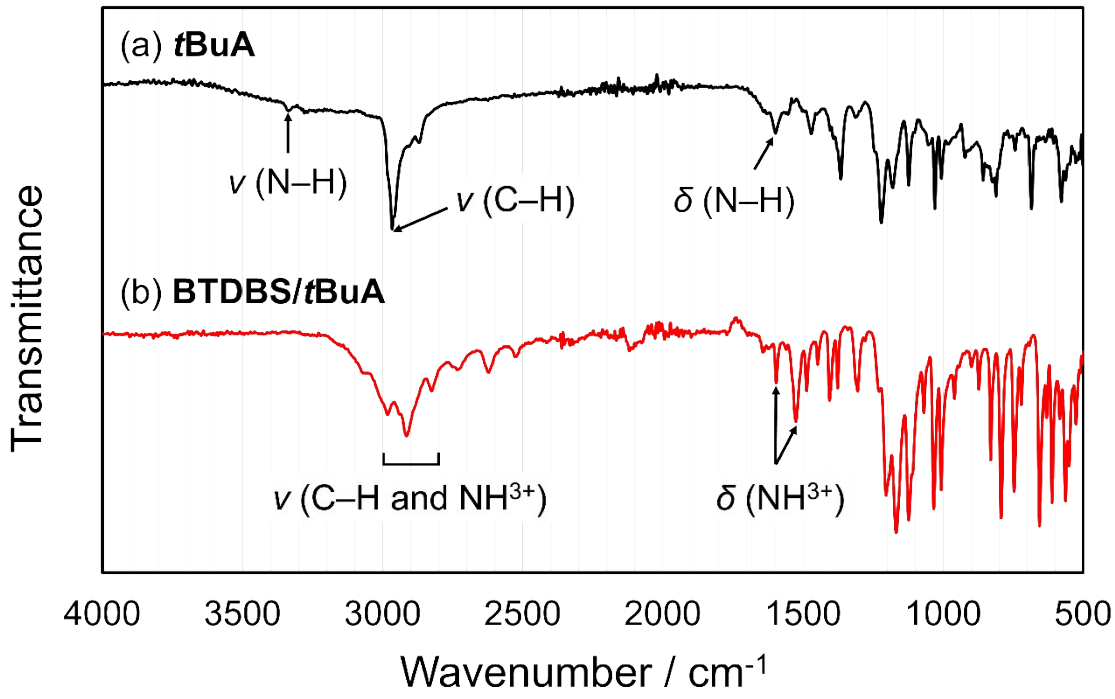

Figure S1. Infrared absorption spectra of (a) ***t*BuA** (black) and (b) **BTDBS/*t*BuA** (red). The weak stretching vibration of N–H (Figure S1, black, *ν*(N–H)) disappeared and the stretching vibration of C–H and NH_3^+ (Figure S1, red, *ν*(C–H and NH_3^+)) in the range of 2800–3000 cm^{-1} and the sharp vending vibration of NH_3^+ (Figure S1, red, *δ*(NH_3^+)) in the range of 1500–1600 cm^{-1} were appeared, which indicated that the amine (NH_2) was protonated by sulfonic acid ($–SO_3H$) to be $–NH_3^+$.

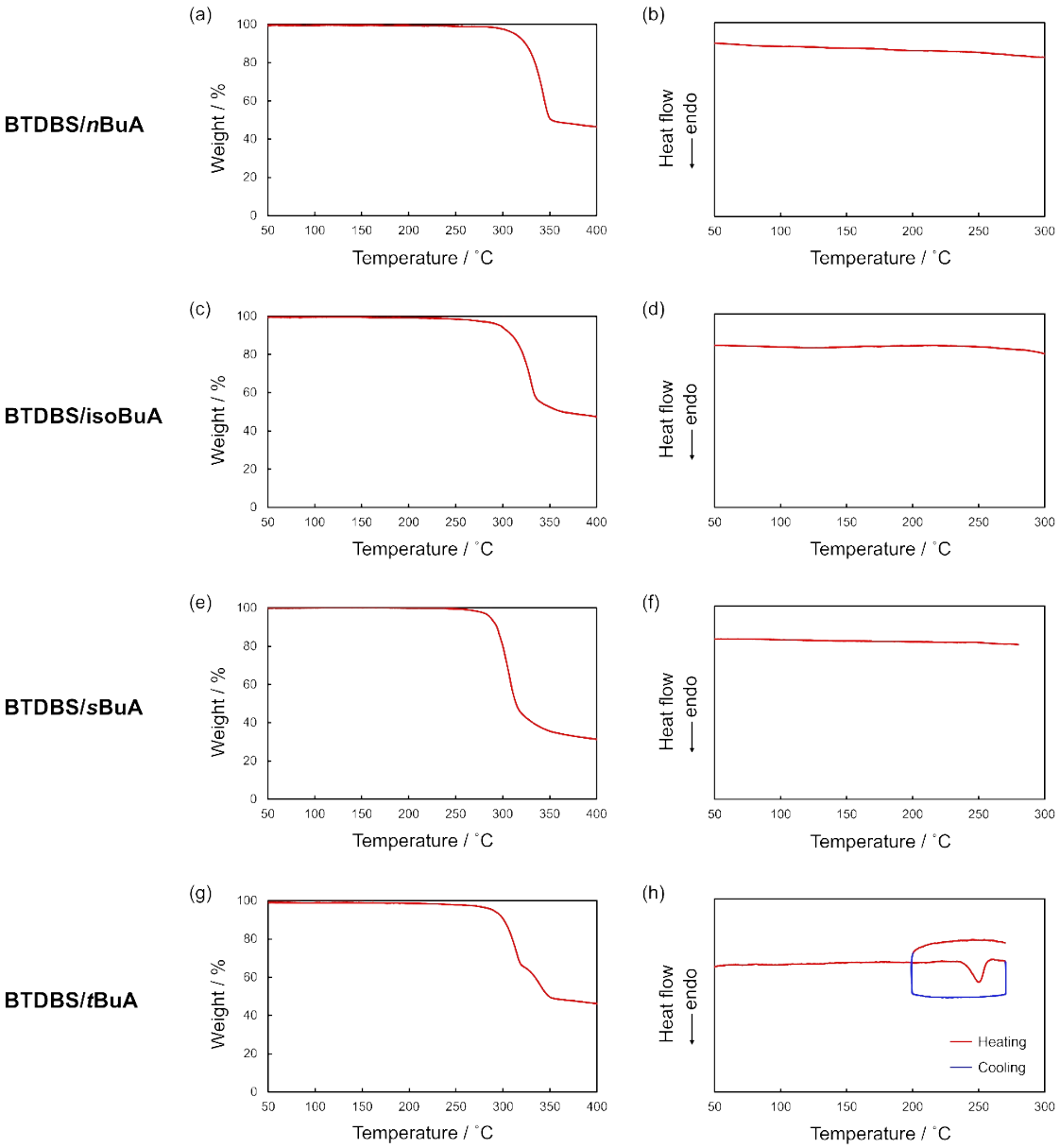

Figure S2. (a, c, e, g) Thermogravimetric analysis (TGA) and (b, d, f, h) differential scanning calorimetry (DSC) of (a, b) **BTDBS/*n*BuA**, (c, d) **BTDBS/isoBuA**, (e, f) **BTDBS/*s*BuA**, and (g, h) **BTDBS/*t*BuA**. The data indicated that all of the organic salts did not have melting point lower than their decomposition temperature at around 250°C.

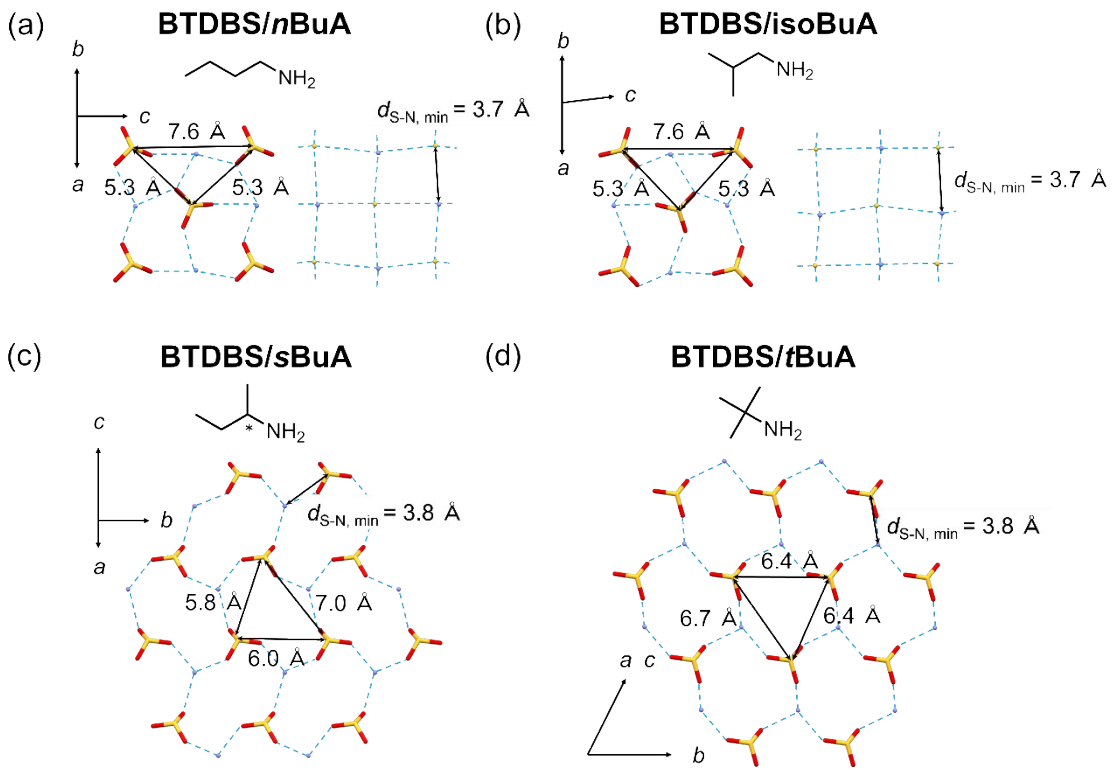

Figure S3. The hydrogen bond networks based on the charge-assisted hydrogen bonding in the crystal structures of (a) **BTDBS/*n*BuA**, (b) **BTDBS/isoBuA**, (c) **BTDBS/*s*BuA** and (d) **BTDBS/*t*BuA**. **BTDBS/*n*BuA** and **BTDBS/isoBuA** had two-dimensional hydrogen-bonding networks, where a sulfonate anion made hydrogen bonds with four ammonium cations, and an ammonium cation made hydrogen bond with four sulfonate anions. This was because three hydrogen atoms of ammonium cations are delocalized (Figures S3a and S3b). The shortest S–N distances ($d_{S\text{-}N,\ min}$) of **BTDBS/*n*BuA** and **BTDBS/isoBuA** were 3.7 Å. **BTDBS/*s*BuA** and **BTDBS/*t*BuA** had two-dimensional hydrogen-bonding networks formed by six-membered hydrogen-bonded rings (Figures S3c and S3d) because of the bulkiness of ***s*BuA** and ***t*BuA**. $d_{S\text{-}N,\ min}$ of **BTDBS/*s*BuA** and

BTDBS/*t*BuA was 3.8 Å, which was almost the same as **BTDBS/*n*BuA** and **BTDBS/isoBuA**. As a result, the shortest sulfone (S) distances being about 0.5 Å longer than those of **BTDBS/*n*BuA** or **BTDBS/isoBuA**, which leads to leaving adjacent disulfonic acids each other.

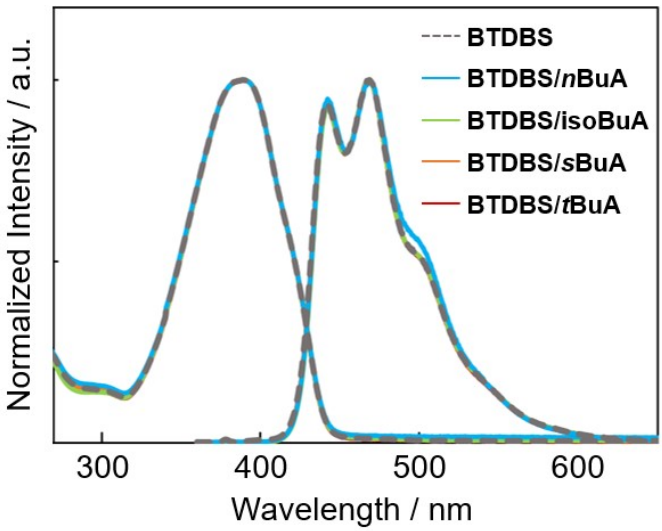

Figure S4. Absorption and emission spectra of **BTDBS** and the organic salts composed of **BTDBS** and various alkylamines in DMSO solution (1.0×10^{-5} M). Excitation wavelength for the emission spectra was 340 nm.

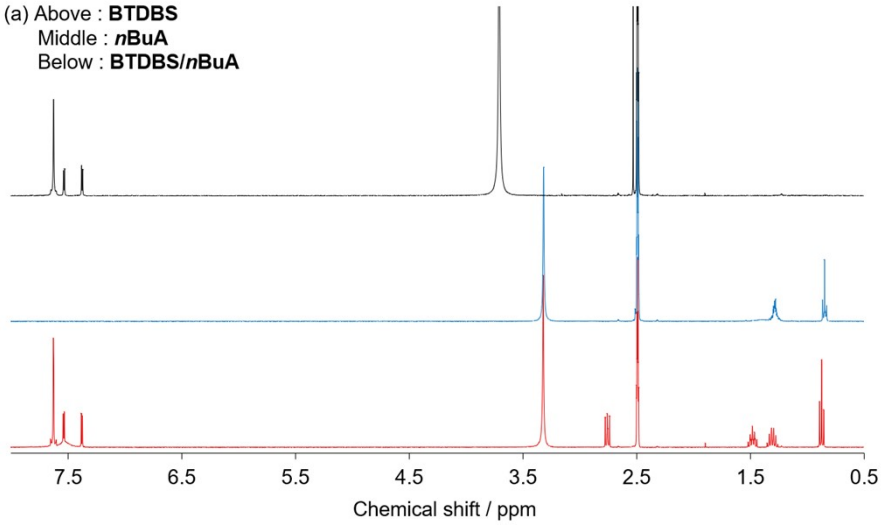
(a) Above : **BTDBS**
Middle : ***n*BuA**
Below : **BTDBS/*n*BuA**
7.5
6.5
5.5
4.5
3.5
2.5
1.5
0.5
Chemical shift / ppm

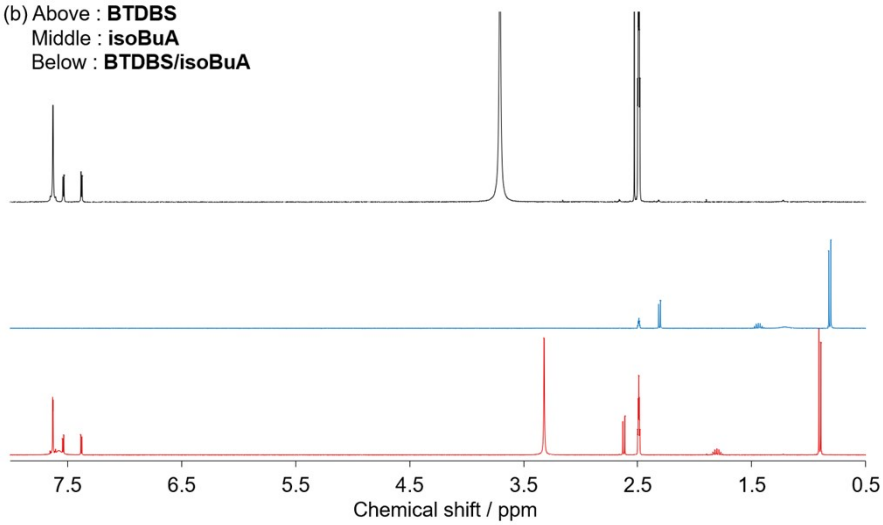
(b) Above : **BTDBS**
Middle : **isoBuA**
Below : **BTDBS/isoBuA**
7.5
6.5
5.5
4.5
3.5
2.5
1.5
0.5
Chemical shift / ppm

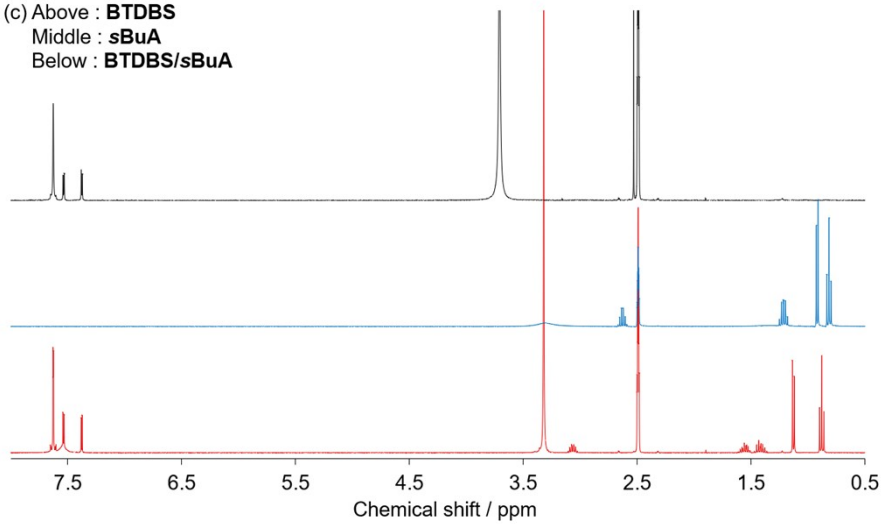
(c) Above : **BTDBS**
Middle : ***s*BuA**
Below : **BTDBS/*s*BuA**
7.5
6.5
5.5
4.5
3.5
2.5
1.5
0.5
Chemical shift / ppm

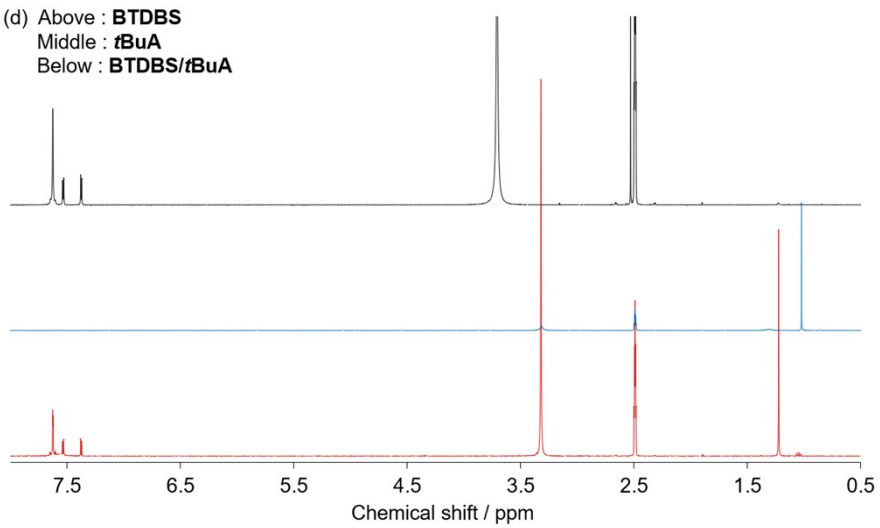

Figure S5. 400 MHz ^{1}H NMR spectra (dimethyl sulfoxide-d_6) of (a) **BTDBS** (black line), ***n*BuA** (blue line), and **BTDBS/*n*BuA** (red line), (b) **BTDBS** (black line), **isoBuA** (blue line), and **BTDBS/isoBuA** (red line), (c) **BTDBS** (black line), ***s*BuA** (blue line), and **BTDBS/*s*BuA** (red line), (d) **BTDBS** (black line), ***t*BuA** (blue line), and **BTDBS/*t*BuA** (red line). The protonation of amines by mixed with **BTDBS** induced the peak shifts of alkyl substituents of amines to the low magnetic field side. Even when **BTDBS** is deprotonated by adding alkylamines, the peaks of the functional part (**BT**) had no change, which indicated that the electron density of **BT** was not changed.

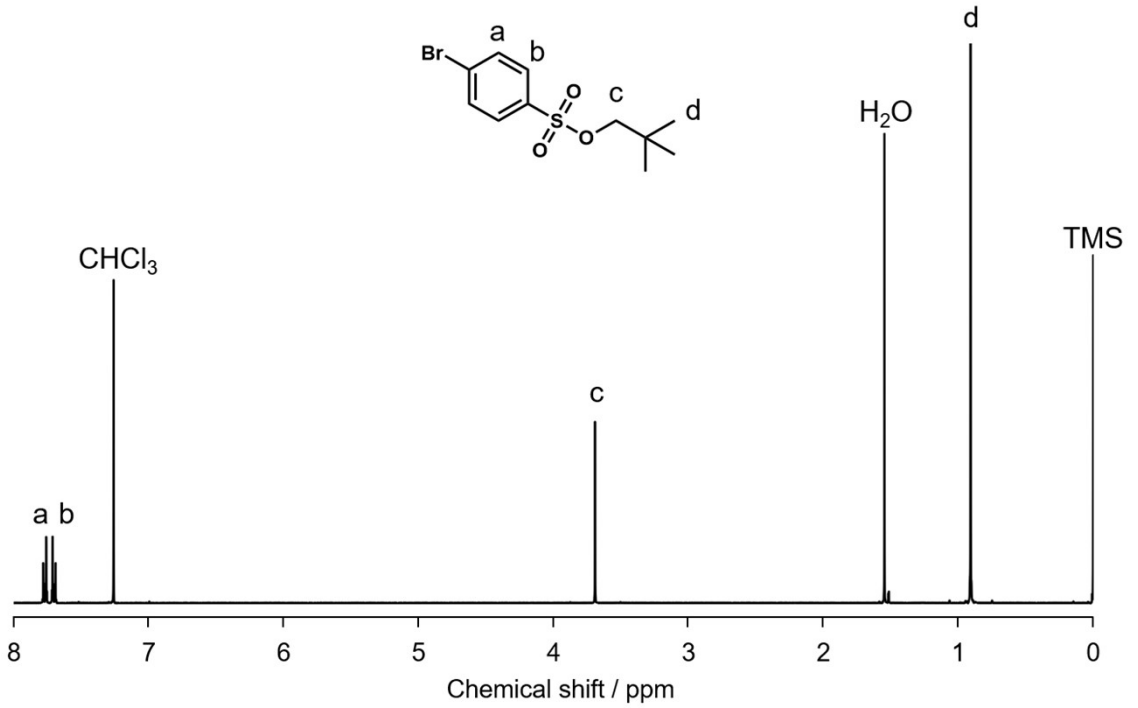

Figure S6. 400 MHz ^{1}H NMR spectrum (chloroform-d_1) of neopentyl 4-bromobenzenesulfonate.

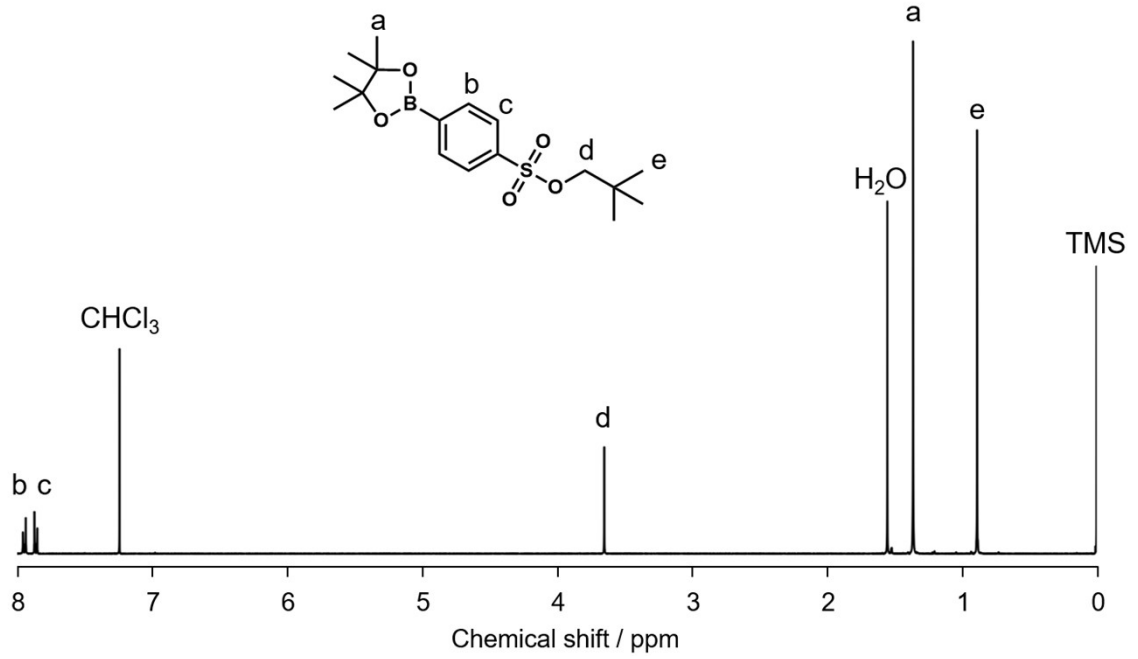

Figure S7. 400 MHz ^{1}H NMR spectrum (chloroform-d_1) of neopentyl 4-(4,4,5,5-tetramethyl-1,3,2-dioxaborolan-2-yl)benzenesulfonate.

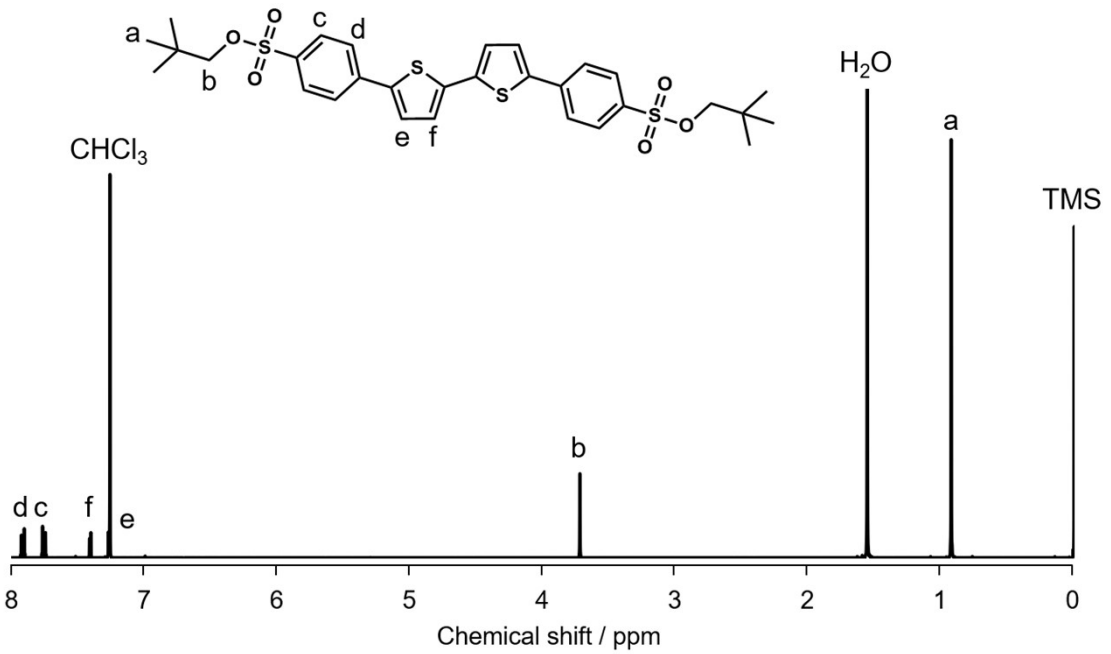

Figure S8. 400 MHz ^{1}H NMR spectrum (chloroform-d_1) of dineopentyl 4,4'-([2,2'-bithiophene]-5,5'-diyl)dibenzenesulfonate.

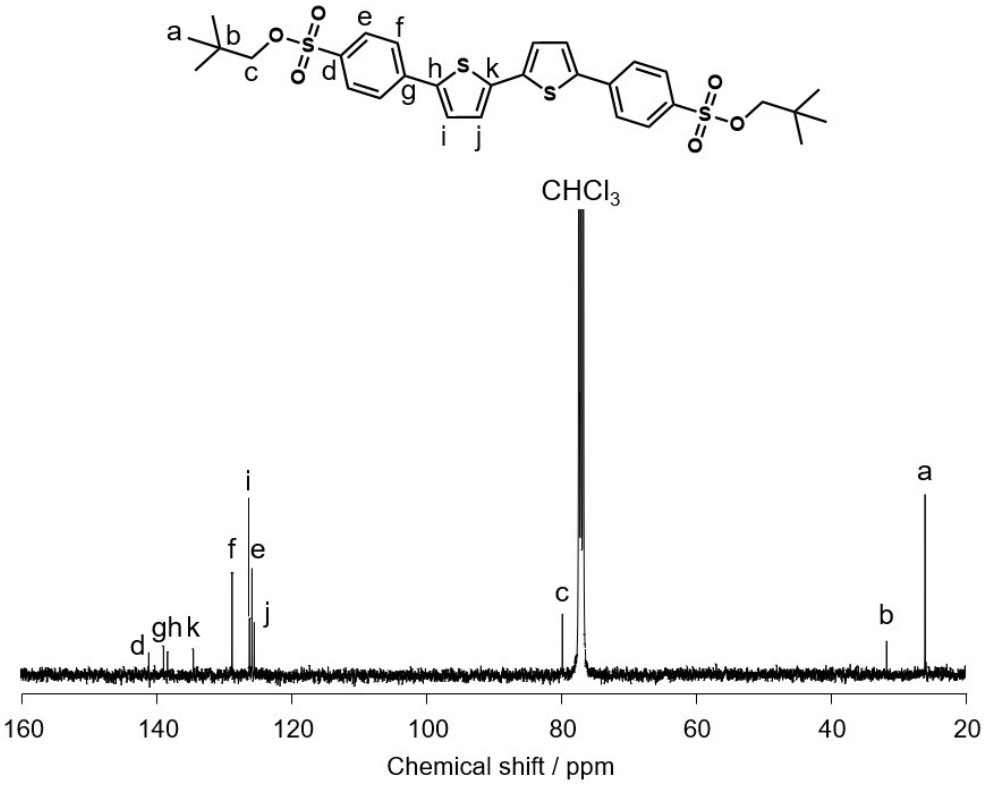

Figure S9. 400 MHz ^{13}C NMR spectrum (dimethyl sulfoxide-d_6) of dineopentyl 4,4'-([2,2'-bithiophene]-5,5'-diyl)dibenzenesulfonate.

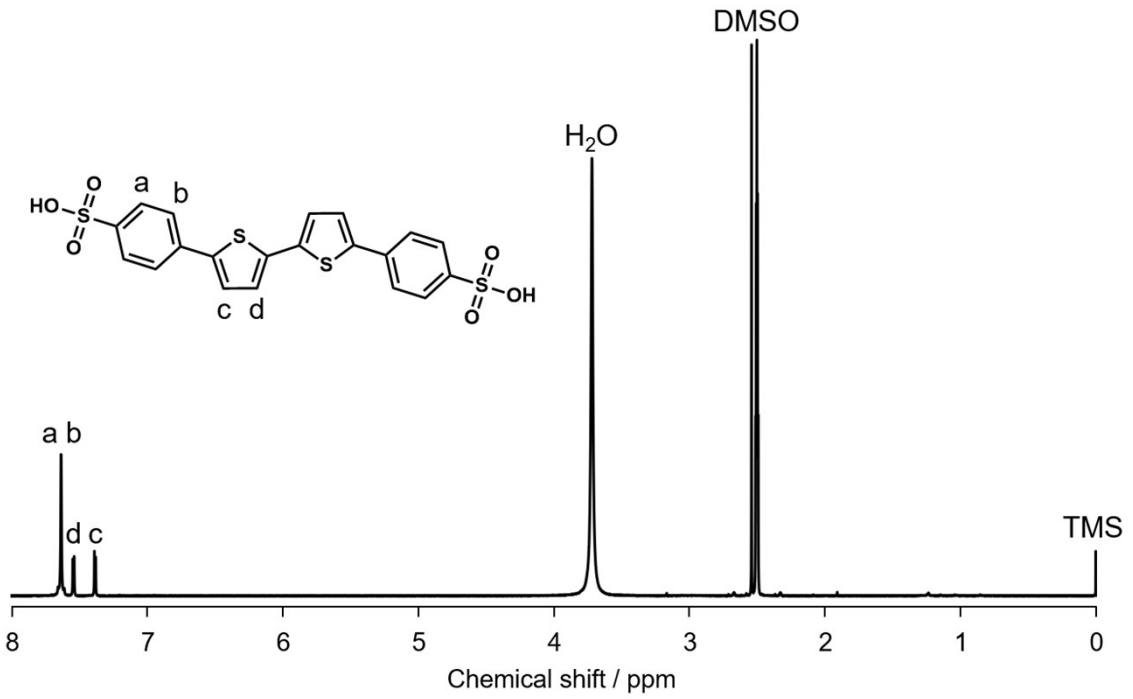

Figure S10. 400 MHz ^{1}H NMR spectrum (dimethyl sulfoxide-d_6) of 4,4'-([2,2'-bithiophene]-5,5'-diyl)dibenzenesulfonic acid (**BTDBS**).

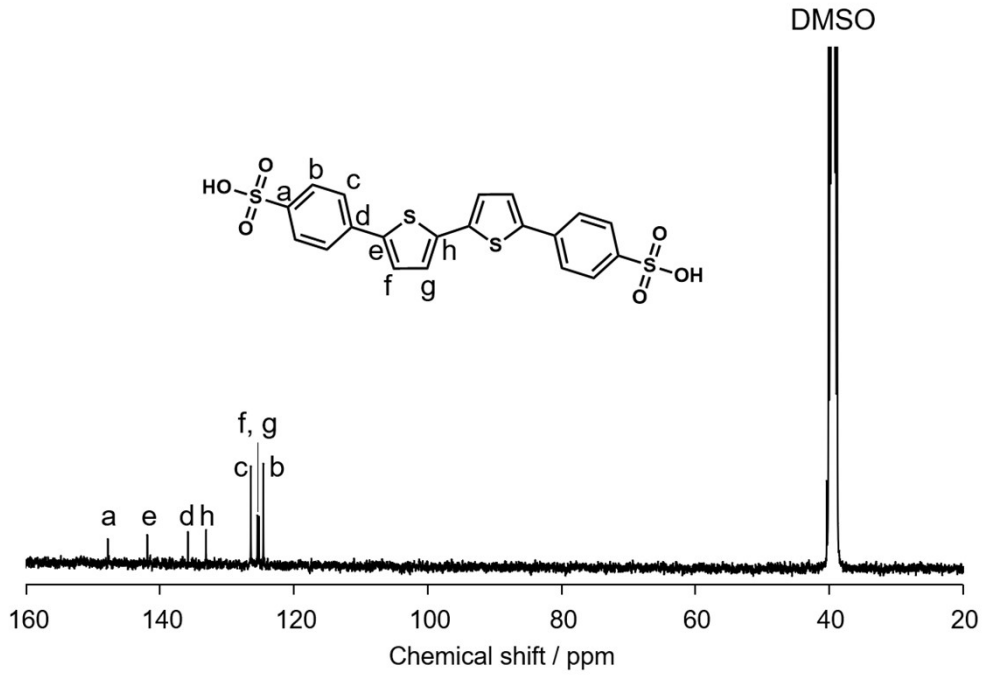

Figure S11. 400 MHz ^{13}C NMR spectrum (dimethyl sulfoxide-d_6) of 4,4'-([2,2'-bithiophene]-5,5'-diyl)dibenzenesulfonic acid (**BTDBS**).

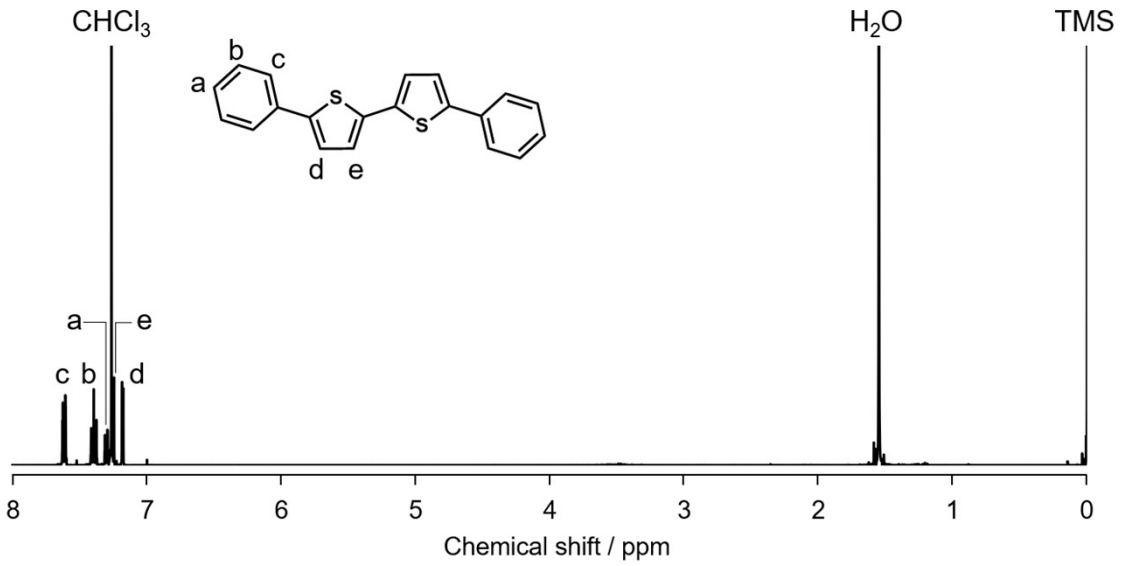

Figure S12. 400 MHz ^{1}H NMR spectrum (chloroform-d_1) of 5,5'-diphenyl-2,2'-bithiophene (**DPhBT**).

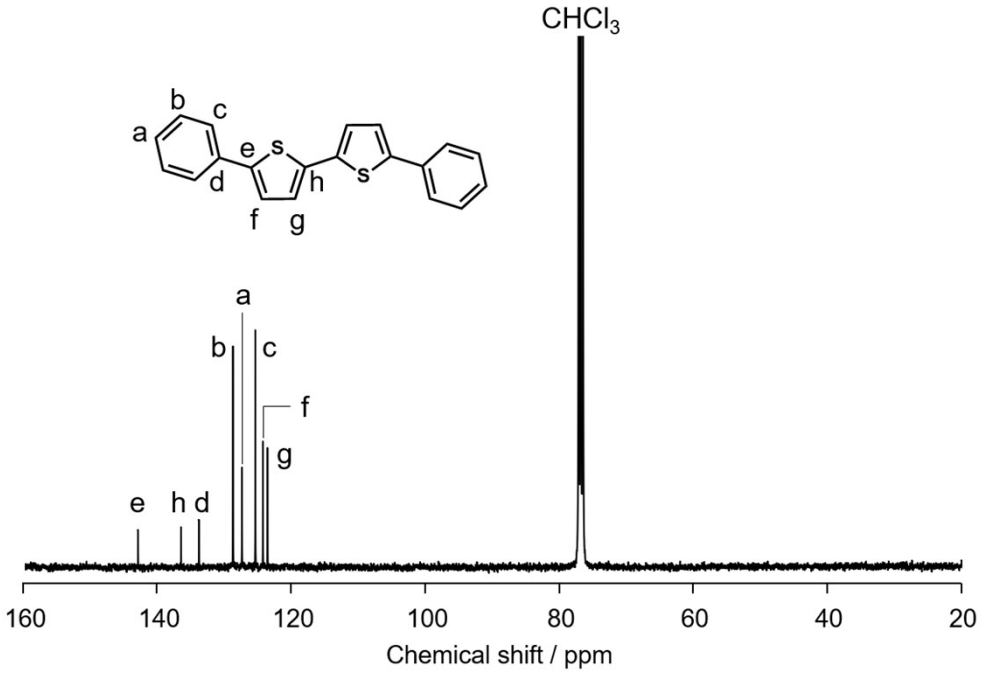

Figure S13. 400 MHz ^{13}C NMR spectrum (chloroform-d_1) of 5,5'-diphenyl-2,2'-bithiophene (**DPhBT**).

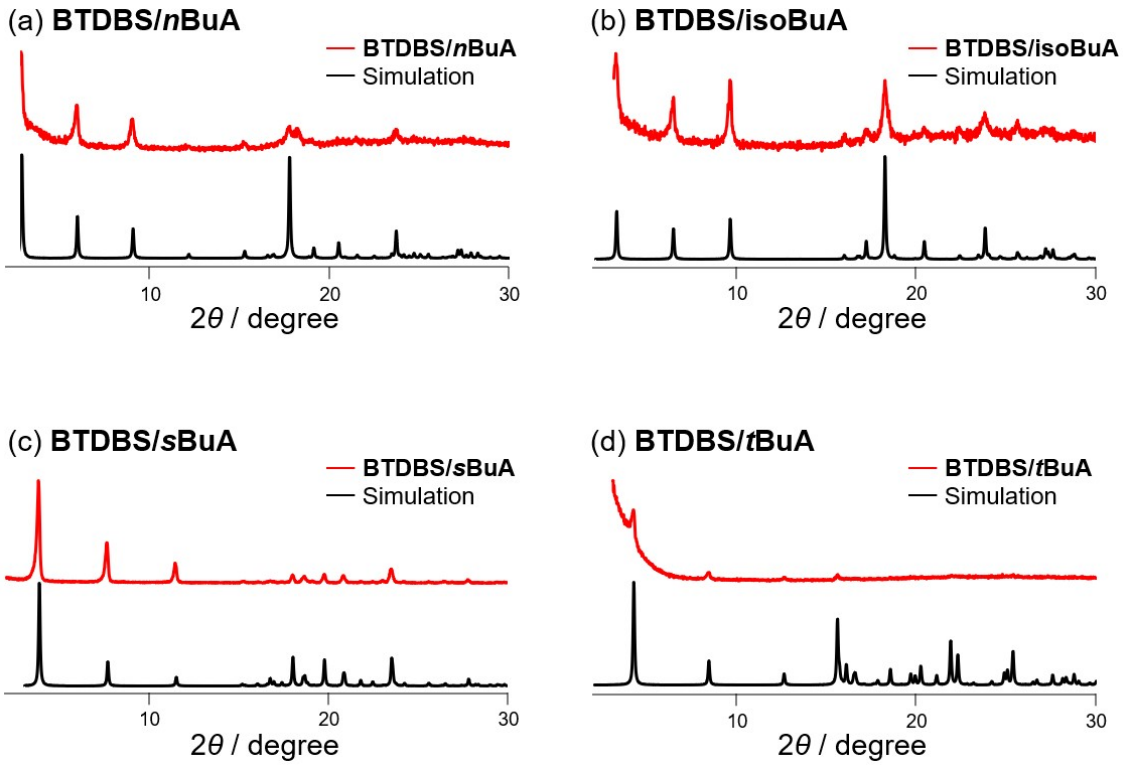

Figure S14. PXRD patterns of (a) **BTDBS/*n*BuA**, (b) **BTDBS/isoBuA**, (c) **BTDBS/*s*BuA**, (d) **BTDBS/*t*BuA**. Simulation (black), after recrystallization (red) from methanol as good solvent and acetonitrile as poor solvent.

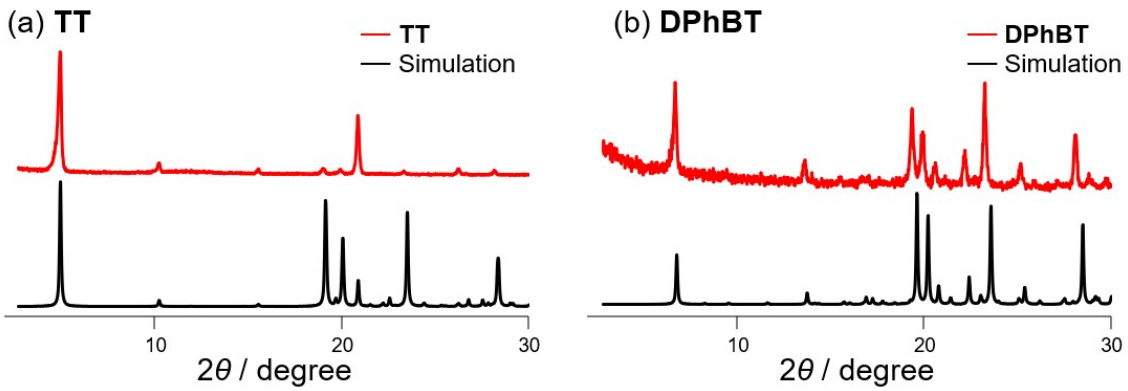

Figure S15. PXRD patterns of (a) **TT**, (b) **DPhBT**. Simulation (black), after recrystallization (red). (a) **TT** was recrystallized from diethyl ether. (b) **DPhBT** was recrystallized from chloroform.

Table S1. Crystal structures of 2,2'-bithiophene[2] (**BT**), α-terthiophene[3] (**TT**), 5,5'-diphenyl-2,2'-bithiophene (**DPhBT**), and 4,4'-([2,2'-bithiophene]-5,5'-diyl)dibenzenesulfonic acid (**BTDBS**) with water and 1,4-dioxane.

Entry	Compound	Functional molecule	Crystal structure[a]	Arrangement of the functional part [a]
1	**BT**		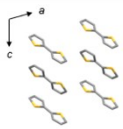	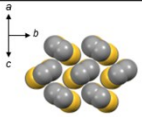 Edge-to-face herringbone
2	**TT**		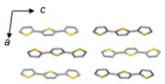	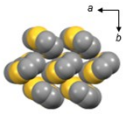 Edge-to-face herringbone
3	**DPhBT**	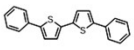	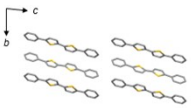	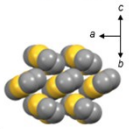 Edge-to-face herringbone
4	**BTDBS**	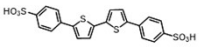	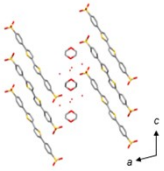	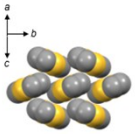 Edge-to-face herringbone

[a] Hydrogen atoms have been omitted for clarity.

Table S2. The crystal structures of the organic salts depending on the number of substituents of the α-carbon of alkylamines.

Amine	***n*BuA** 	***s*BuA** 	***t*BuA** 
The number of substituents of the α-carbon of alkylamines	1	2	3
Crystal structure of the organic salt[a]	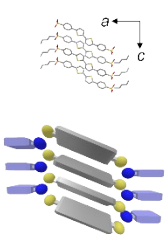	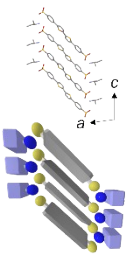	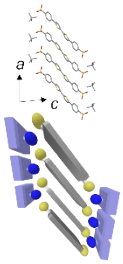
θ_{tilt}	62.9°		39.4°
$\theta_{dihedral}$	51.8°		0°

[a] Hydrogen atoms have been omitted for clarity.

Table S3. Solid-state luminescence properties of α-terthiophene (**TT**) and 5,5'-diphenyl-2,2'-bithiophene (**DPhBT**).

Entry	Compound	Arrangement of the functional part	$\lambda_{ex,\,max}$ [nm][a]	$\lambda_{em,\,max}$ [nm][b]	Φ_F [c]	λ_{em} [nm]	τ_F [ns][d]
1	**TT**	Edge-to-face herringbone	460	479	0.03	455	0.04 (100 %)
						479	0.11 (63 %), 0.50 (37 %)
						508	0.34 (12 %), 0.51 (88 %)
						560	0.51 (97 %), 1.12 (3 %)
2	**DPhBT**	Edge-to-face herringbone	445	550	0.05	522	0.81 (100 %)
						550	0.82 (100 %)
						590	0.85 (100 %)

[a] Maximum wavelengths of the fluorescence excitation spectra monitored at λ_{em}. [b] Maximum wavelengths of fluorescence emission spectra excited at 340 nm. [c] Absolute fluorescence quantum efficiencies. [d] Fluorescence lifetimes excited at 352 nm.

Table S4. Crystallographic parameters of the organic salts.

	BTDBS/*n*BuA	**BTDBS/isoBuA**	**BTDBS/*s*BuA**	**BTDBS/*t*BuA**
fomula	$C_{28}H_{36}N_2O_6S_4$	$C_{28}H_{36}N_2O_6S_4$	$C_{28}H_{34}N_2O_6S_4$	$C_{14}H_{18}NO_3S_2$
fw	624.83	624.83	622.81	312.41
crystal system	monoclinic	monoclinic	monoclinic	triclinic
space group	$P2_1/c$	$P2_1/c$	$P2_1/c$	P-1
a [Å]	28.773(4)	27.9234(7)	23.2637(8)	6.3519(6)
b [Å]	7.4823(5)	7.4749(2)	6.0279(2)	6.3675(5)
c [Å]	7.5607(5)	7.6043(2)	11.1259(3)	21.2470(11)
α [deg]	90	90	90	86.182(5)
β [deg]	91.416(9)	94.855(3)	97.013(3)	83.257(6)
γ [deg]	90	90	90	63.396(9)
V [Å^3]	1627.2(3)	1581.51(7)	1548.53(9)	762.96(12)
Z	2	2	2	2
T [K]	293	293	293	293
R_1 [$I>2\sigma(I)$]	0.0933	0.0530	0.0469	0.0677
Rw [all data]	0.2209	0.1326	0.1404	0.2030
CCDC no.	2152669	2153387	2153395	2153396

Table S5. Crystallographic parameters of **DPhBT** and **BTDBS**.

	DPhBT	**BTDBS**
fomula	$C_{20}H_{14}S_2$	$C_{20}H_{30}O_{12}S_4$
fw	318.43	638.72
crystal system	triclinic	monoclinic
space group	*P*-1	$P2_1/c$
a [Å]	5.68780(10)	16.8387(11)
b [Å]	7.86580(10)	6.0329(4)
c [Å]	16.9636(2)	13.8772(10)
α [deg]	86.3680(10)	90
β [deg]	89.9800(10)	102.928(7)
γ [deg]	89.8680(10)	90
V [Å^3]	757.410(19)	1374.00(17)
Z	2	2
T [K]	213	213
R_1 [$I>2\sigma(I)$]	0.0594	0.0640
*R*w [all data]	0.1440	0.1816
CCDC no.	2153473	2153474

References

1. W. Qu, X. Zhu, J. Chen, L. Niu, D. Liang, X. Fan, Z. Shen and Q. Zhou, *Macromolecules*, 2014, **47**, 2727-2735.
2. G. J. Visser, G. J. Heeres, J. Wolters and A. Vos, *Acta Crystallographica Section B Structural Crystallography and Crystal Chemistry*, 1968, **24**, 467-473.
3. F. Van Bolhuis, H. Wynberg, E. E. Havinga, E. W. Meijer and E. G. J. Staring, *Synth. Met.*, 1989, **30**, 381-389.